Cross-linker Control of Vitrimer Flow

Bassil M. El-Zaatari, Jacob S. A. Ishibashi and Julia A. Kalow*

Department of Chemistry, Northwestern University, Evanston, IL 60208 USA

*email: jkalow@northwestern.edu

Abstract

Vitrimers are a class of covalent adaptable networks (CANs) that undergo topology reconfiguration via associative exchange reactions, enabling reprocessing at elevated temperatures. Here, we show that the use of an associative mechanism additionally enables decoupling of stiffness and stress relaxation. Guided by calculated activation barriers, we prepared a series of cross-linkers with varying reactivity for the conjugate addition—elimination of thiols in a PDMS vitrimer, and demonstrate modulation of stress relaxation rate while maintaining constant stiffness. Surprisingly, despite a wide range of stress relaxation rates, we observe that the flow activation energy of the bulk material is independent of the cross-linker structure. Superposition of storage and loss moduli from frequency sweeps can be performed for different cross-linkers, indicating the same exchange mechanism. We show that we can mix different cross-linkers in a single material in order to further modulate the stress relaxation behavior.

Introduction

The incorporation of reversible linkages within polymer chains or junctions creates dynamic networks that can achieve desirable characteristics such as self-healing, recyclability, and stimuli-responsivity.[1–5] The rate at which networks dissipate applied

stress, or stress relaxation, governs how quickly self-healing occurs at a given temperature. To fine-tune the rate of stress relaxation, researchers have turned to reversible metal-ligand interactions, [6] host-guest complexation, [7] protein-protein interactions,[8] and dynamic covalent bonds.[9–11] All of these systems undergo cross-link exchange through dissociative mechanisms, meaning that the cross-link must be broken before a new cross-link can form (Figure 1a). An ongoing challenge in the field is rationally decoupling stiffness, which is governed by crosslink density, and stress relaxation.[12] In supramolecular networks, Craig and Scherman were able to quantitatively relate stress relaxation rates to cross-link dissociation.[6,7] However, in order to tune stress relaxation without affecting the crosslink density, these researchers needed to identify combinations of exchange partners with identical binding constants but different dissociation rates.

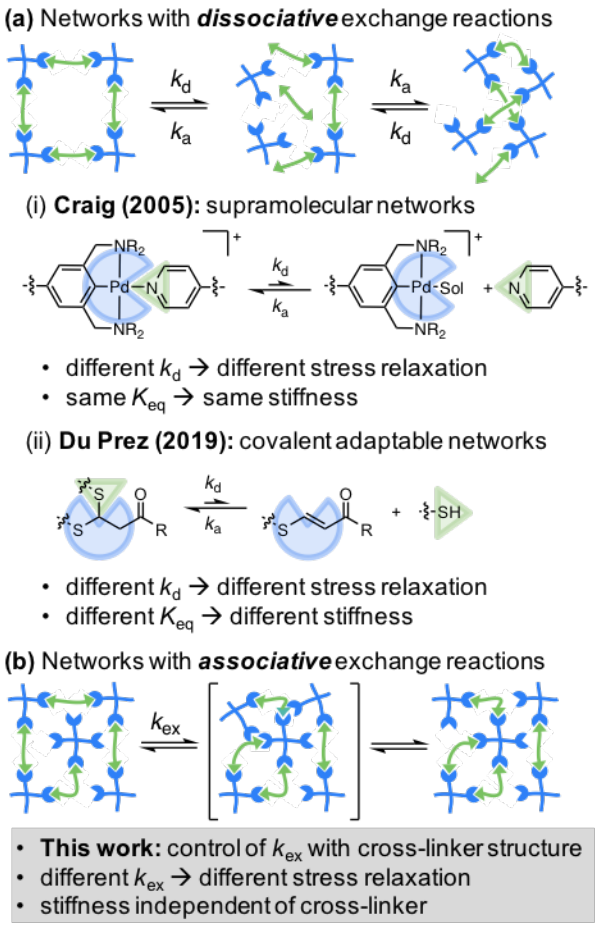

Figure 1. Overview of dissociative and associative dynamic networks. **(a)** Dissociative exchange mechanism and examples in which the stress relaxation was tuned by modification of the R group: (i) metal-ligand supramolecular exchange and (ii) reversible thiol-Michael addition/elimination. **(b)** Associative exchange mechanism and consequences for network properties.

In this paper, we show that small structural modifications to cross-links in *associative* covalent adaptable networks (CANs), or vitrimers,[13–15] offer control over stress relaxation independent of stiffness (Figure 1b). In contrast to CANs that proceed through dissociative processes, vitrimers maintain their cross-linked structure during swelling and heating, but can still be remolded and repaired.[5] A wide array of associative dynamic covalent chemistries have been employed in vitrimers, including transesterification,[16–18] olefin metathesis,[19,20] dioxaborolane exchange, [21–23], silyl ether exchange[24] and several others.[25–34] Despite the number of reactions studied, there are few systematic studies that examine the effect of cross-linker structure on vitrimer properties.[25,27,35]

It is common practice to relate the rate and activation energy of the molecular exchange reaction to a vitrimer's stress relaxation behaviour.[27] Strategies to control the rate of associative exchange reactions in networks include pH, [36] catalysts,[37] and acid/base additives.[25] Notably, Leibler and co-workers demonstrated that changing the catalyst type and concentration affects flow activation energies for ester-based vitrimers. [38] Bates and co-workers identified a surprising inverse relationship between the pKa of Brønsted acid catalysts and flow activation energy. [39]

Catalysts can suffer from leaching and deactivation, motivating our interest in catalyst-free exchange reactions for vitrimers. We previously demonstrated that the conjugate addition–elimination of thiols to a Meldrum's acid-derived acceptor40 in a PDMS vitrimer enables at least ten reprocessing cycles without loss of properties (Scheme 1).[41] Here, we synthesize a series of conjugate acceptor cross-linkers and compare their reactivity in vitrimers. Key differences in reactivity can be rationalized based on calculated transition states. We obtain vitrimers exhibiting a wide range of stress relaxation times, spanning

over 4 orders of magnitude, with nearly identical stiffnesses. We can superimpose frequency sweeps for three distinct cross-linkers with a horizontal shift factor, suggesting that relaxation occurs through a common mechanism. Finally, we can further tune the stress relaxation profiles by mixing cross-linkers with different reactivities into single networks. This study revealed two new cross-linkers that enable significantly faster stress relaxation compared to the original Meldrum's acid-derived acceptor.

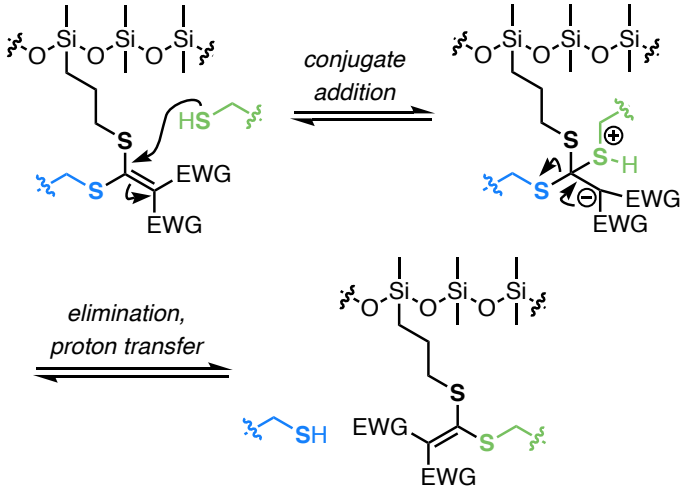

Scheme 1. Mechanism of the conjugate addition–elimination exchange reactions in the elastomeric PDMS vitrimer studied here.

Results and Discussion

Vitrimers were prepared using commercially available polydimethylsiloxane (PDMS) grafted with 13-17 mol% propylthiol groups, as previously described.[41] In addition to the original Meldrum's acid-based cross-linker (**MA**) and a commercial malonitrile derivative (**CN**), four cross-linkers were synthesized by base-assisted nucleophilic addition of the 1,3-dicarbonyl compound to CS_2, followed by methylation (Figure 2a). These cross-linkers are named based on the dicarbonyl structures: cyclohexanedione (**CY**), barbituric acid (**BA**), indanedione (**IND**), and diphenylpropanedione (**DP**) (Figure 2b). To form the vitrimers, the cross-linkers were combined with thiol-grafted PDMS at 2 mol% relative to

the siloxane repeat units. The mixtures were heated (100–150 ºC) to induce gelation and were reprocessed prior to testing to ensure homogenous samples (see Electronic Supporting Information (ESI) for additional information).

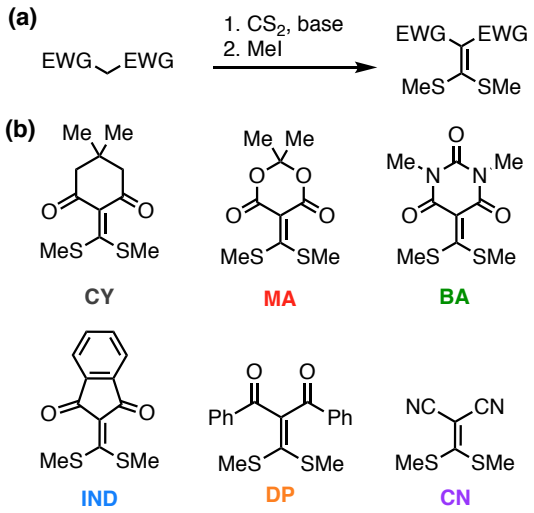

Figure 2. (a) General synthesis for cross-linkers used in the study. **(b)** Structures of different cross-linkers used in the study.

To predict differences in exchange rates between the different cross-linkers, we performed DFT calculations (B3LYP/def-TZVP gas phase.) The initial conjugate addition step is rate limiting, so transition states for this step were calculated and minimized. The temperature used for the calculations was 135 ºC. For the cyclic cross-linkers (**MA**, **IND**, **BA**, **CY**), closed, six-membered transition states were located (Figure 3 and Figure S11). In normal reaction media, mobile solvent molecules or additives can aid the addition of thiols to Michael acceptors by acting as proton transfer agents.[40] However, in the nonpolar environment of the PDMS matrix, in which our polymer network is formed, it is reasonable to invoke the participation of an internal base (i.e., the carbonyl of the cross-linker) to mediate proton transfer from the thiol in a closed transition state. The lowest activation barrier belongs to **CY** (+112 kJ/mol), followed by **BA**, **IND** and **MA**, which have similar calculated $\Delta G^{\ddagger}$ values to each other (Figure 3).

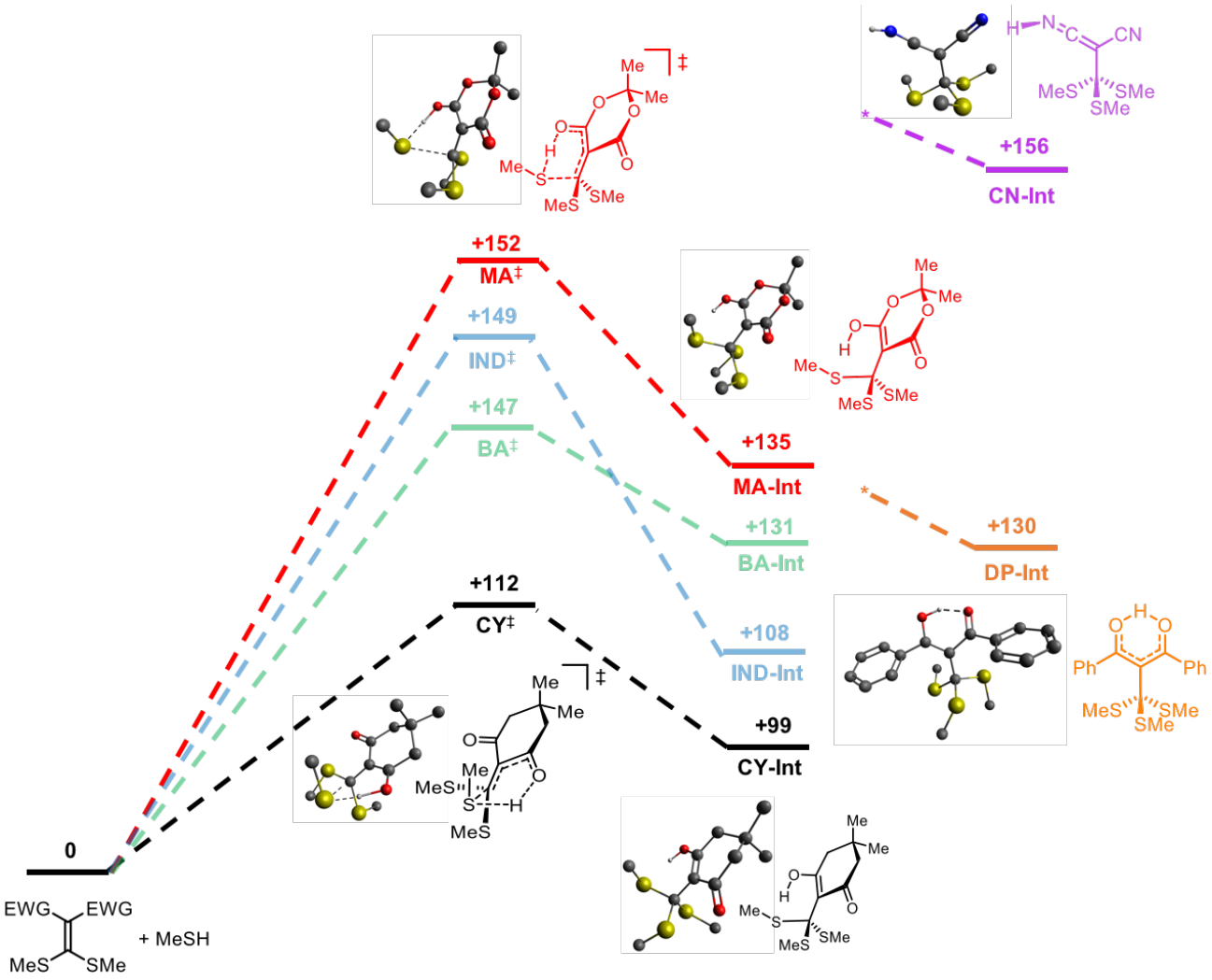

Figure 3. Calculated transition states and intermediate energies for the cross-linkers (energies are not drawn to scale). Representative optimized cyclic transition state and intermediates for the conjugate addition of methanethiol to **MA** and **CY**, and intermediates for **CN** and **DP**, are shown. H atoms on CH_3 groups are omitted for clarity. *No cyclic transition states were located for **DP** and **CN**.

Tetrahedral intermediates for the acyclic cross-linkers **DP** and **CN** orient the proton away from the thiols, and correspondingly, no closed transition states were located. The N_{sp} lone pairs on each nitrile of **CN** point away from the site of nucleophilic attack. The bond rotations required in **DP** to accommodate a cyclic transition state would likely result in unfavourable steric interactions (Figures S10-S12). Thus, the acyclic cross-linkers lack an internal base to accelerate the exchange process.

To compare the effect of cross-linker structure in vitrimers, stress relaxation experiments were performed using shear rheology (Figure 4a; for additional details, see ESI). The vitrimer networks are named based on the cross-linker used (e.g., **CY-Net**). The rate of the relaxation process can be characterized with respect to a characteristic relaxation time constant, τ*. Assuming Maxwell behaviour, τ* is defined as the time needed for the relaxation modulus to decrease to 1/e of its initial value. The τ* values for this series of cross-linkers span 4 orders of magnitude, following the trend **CY** < **BA** < **IND** ~ **MA** << **CN** ~ **DP** (Figure 4b). This trend is consistent with the calculated $\Delta G^{\ddagger}$ values, suggesting that the stress relaxation in these materials is directly correlated to the exchange kinetics. The wide range in stress relaxation rates was accompanied by modest differences in stiffness. The rubbery plateau moduli of these networks at 150 ºC were determined by frequency sweeps between 100 and 1 rad/s and were found to be similar for all cross-linkers, ranging between 100 and 130 kPa (Figure 4b). The similarity of the plateau moduli suggest that cross-link density is not affected by the structure of the cross-linker, consistent with an associative mechanism.

The flow activation energy (E_a) is determined by measuring τ* as a function of temperature based on the Arrhenius relationship (equation 1):

$$\tau^* = \tau_0 e^{\frac{-E_a}{RT}} \quad (1)$$

where R is the ideal gas constant, T is the temperature, and τ_0 is a pre-exponential factor.

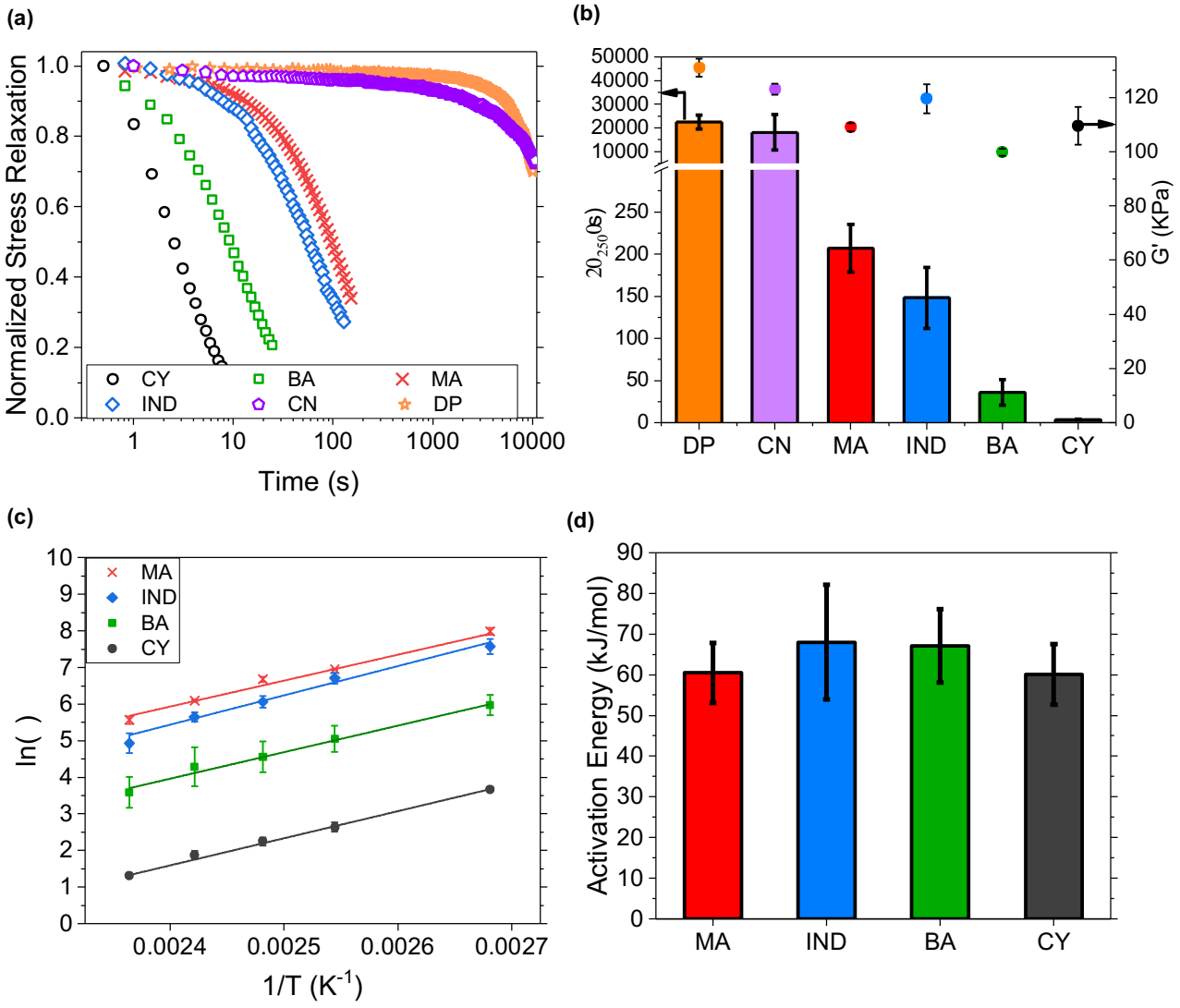

Figure 4. Mechanical properties of the networks. **(a)** Representative normalized stress relaxation profiles at 150 ºC. **(b)** Calculated τ* values for the different cross-linked vitrimers (bar graph, left axis) and their rubbery plateau moduli at the same temperature (circle symbols, right axis). Error bars are based on student's t distribution. The τ* values calculated using 1/e of the relaxation modulus for the cyclic cross-linkers and by extrapolating a stretched exponential function for the acyclic cross-linkers (see ESI for more detail). **(c)** Arrhenius plots for stress relaxation of networks derived from the cyclic cross-linkers. **(d)** Calculated flow activation energies for the networks. Error bars are based on mean square error analysis of the fitted slopes.

Surprisingly, the flow activation energies calculated for the different cyclic cross-linkers were within experimental error, with their averages ranging between 60 and 68 kJ/mol (Figures 4c and 4d). Instead, the difference in relaxation times is driven by the pre-exponential factor, τ_0, represented by the change in y-intercept (Table S9). τ_0 has been defined as the relaxation time at infinite temperature, but the physical underpinnings of this

value in vitrimers are not well understood.[5] For the acyclic cross-linkers, the experimentally accessible temperature range was too narrow for an accurate Arrhenius analysis.

Activation energy values represent the temperature sensitivity of a process, and not the absolute kinetics. Rational strategies to tune the flow activation energy E_a and the pre-exponential factor τ_0 are necessary to guide optimization of vitrimer properties. For example, to minimize creep at service temperatures but enable flow at elevated temperatures without decomposition, high E_a is desirable.[25] In ester and vinylogous urethane vitrimers, catalysts modulate relaxation times by changing both E_a and τ_0.[24,25,35] Our results show that the absolute rate of stress relaxation can be modulated without affecting the temperature dependence by changing the structure of the cross-linker.

Some vitrimer systems exhibit a change in exchange mechanism as a function of temperature or additives.[42,43] We sought to confirm that changing the structure of the cross-linker in the vitrimer did not influence the mechanism of exchange. Typically, time-temperature superpositions (TTS) of frequency sweeps are used in polymer rheology to determine if the relaxation processes scale as a function of temperature. In order to determine if the relaxation processes in our vitrimers scale as a function of cross-linker reactivity, a time-cross-linker superposition (TCLS) was constructed at 150 ºC (3% strain, 0.01–100 rad/s) for representative cross-linkers (Figure 5). The networks in this study contained 1.25 mol% of the cross-linker, which allowed access to the terminal regime. We were able to superimpose the **CY-Net** and **BA-Net** storage (G') and loss (G'') moduli curves onto the reference **IND-Net** data using only horizontal shift factors. This superposition suggests that the mechanism of stress relaxation is indeed identical for the

cyclic cross-linkers; the only difference between samples is how fast or slow the collective relaxation process is.

The horizontal shift factors (α_T) were calculated from the crossover frequencies (ω_c), which are inversely related to the characteristic stress relaxation times τ* for an ideal Maxwell material (equation 2).

$$\alpha_T = \frac{\omega_{c,IND}}{\omega_{c,crosslinker}} = \frac{\tau^*_{crosslinker}}{\tau^*_{IND}} \quad (2)$$

Furthermore, a vertical shift factor was not required, and the rubbery plateau moduli of the samples with 1.25 mol% cross-linker ranged between 8 and 11 kPa, again demonstrating that an associative exchange mechanism can decouple stiffness and stress relaxation.

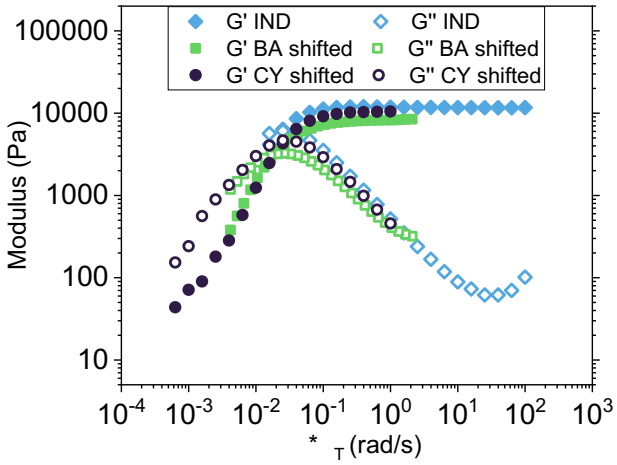

Figure 5. Time—cross-linker superposition for both the storage (G') and loss (G'') moduli of networks with three different cross-linkers (**IND, BA**, and **CY**). IND was used as the reference.

For dissociative reversible networks, mixing cross-linkers with different relaxation rates modulates stress relaxation profiles.[12,44,45] Analogous mixed-cross-linker studies have not been performed in associative networks, so the effect on stress relaxation is unknown. We

formulated three separate samples based on binary mixtures of cross-linkers (1 mol% each): **CY/MA-Net**, **BA/MA-Net**, and **BA/DP-Net**. Stress relaxation measurements were carried at 140 ºC (Figure 6a). As expected based on the stress relaxation of the single cross-linker networks, the stress relaxation times follow the trend **CY/MA-Net** < **BA/MA-Net** < **BA/DP-Net**. Each stress relaxation profile is intermediate to those of its individual cross-linker counterparts. The shape of the normalized stress relaxation curves for the mixed systems indicate additional complexity. The **BA/MA-Net** relaxation data could be fitted to an ideal Maxwell model, whereas **CY/MA-Net** and **BA/DP-Net** relaxation deviated from ideal Maxwell behaviour, suggesting that multiple relaxation modes are operative (Figure 6a and Figure S9). The continuous relaxation spectra were then extracted from the stress relaxation data (see ESI for more detail). Interestingly, three relaxation modes were obtained for the **CY/MA-Net** sample (Figure 6b). The **BA/DP-Net** sample showed an onset of a second relaxation mode at longer times. In contrast, only a single relaxation mode for **BA/MA-Net** was obtained (Figure 6b).

We conclude that combinations of cross-links with relatively similar relaxation rates (**BA** and **MA**) follow Maxwell behaviour with a single relaxation mode, while combinations with very different relaxation rates (**CY** and **MA**, or **BA** and **DP**) exhibit distinct modes for each cross-linker, in addition to an intermediate mode (only the fast and beginning of the intermediate mode are in the experimentally observable time scale for **BA/DP-Net**). These results are contrasted to dissociative systems: mixed boronic ester cross-links resulted in single unimodal Maxwell distributions,[44] and mixed metal-ligand[12] and protein-protein cross-links[45] showed a distinct relaxation mode for each component.

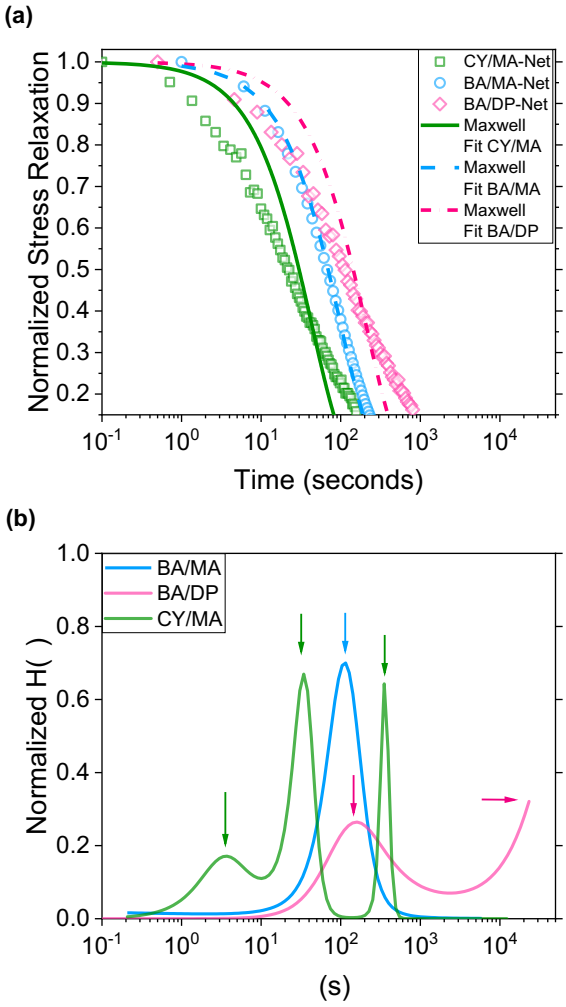

Figure 6. (a) Normalized stress relaxation data for **CY/MA-Net**, **BA/MA-Net**, and **BA/DP-Net** at 140 ºC. An idealized Maxwell fit was performed on each of the relaxation profiles. **(b)** Normalized relaxation spectrum H(τ), as a function of relaxation time, τ for the three mixed networks. Arrows indicate the maxima of the normalized H(τ) peaks.

Conclusions

Decoupling spatial and temporal structure is a fundamental challenge in soft materials.[44] Here, we show that the associative exchange reactions used in vitrimers enable synthetic control over stress relaxation independent of stiffness. The rate of stress relaxation in PDMS vitrimers was shown to be dependent on the structure and reactivity of the electrophilic cross-linker, while maintaining the same exchange mechanism and crosslink density. Thus, we can tune the stress relaxation profile of the network by several orders of

magnitude with only small perturbations to the stiffness. The flow behavior may be further modulated by mixing cross-linkers with distinct rates; this is the first example of mixed-crosslinker studies in a CAN with an associative mechanism. Our results suggest that in vitrimers with a common exchange mechanism, changing the structure of the exchange partner can dramatically alter the stress relaxation rate without altering the flow activation energy. This result is contrasted to the effect of catalysts, which are more commonly used to accelerate flow in vitrimers, and do so by lowering the flow activation energy. These insights will enable rational optimization of vitrimers to strike the balance between limiting creep and accelerating repair.

Conflicts of interest

There are no conflicts to declare.

Acknowledgements

The authors gratefully acknowledge the Center for Chemistry of Molecularly Optimized Networks (NSF CHE-1832256) for funding. This work made use of the Integrated Molecular Structure Education and Research Center at Northwestern, which has received support from the NIH (S10-OD021786-01). Rheological measurements were performed at the Materials Characterization and Imaging Facility which receives support from the MRSEC Program (NSF DMR-1720139) of the Materials Research Center at Northwestern University. The authors additionally thank Dr. Scott Danielson, Prof. Michael Rubinstein, and Prof. Stephen Craig (Duke University) for helpful discussion as well as Mukund Kabra (University of Delaware) for help executing Python code.

Notes and references

1. J. M. Lehn, *Chem. Soc. Rev.*, 2007, **36**, 151–160.
2. C. J. Kloxin and C. N. Bowman, *Chem. Soc. Rev.*, 2013, **42**, 7161–7173.
3. Y. Jin, C. Yu, R. J. Denman and W. Zhang, *Chem. Soc. Rev.*, 2013, **42**, 6634–6654.
4. W. Zou, J. Dong, Y. Luo, Q. Zhao and T. Xie, *Adv. Mater.*, 2017, **29**, 1606100.
5. G. M. Scheutz, J. J. Lessard, M. B. Sims and B. S. Sumerlin, *J. Am. Chem. Soc.*, 2019, 141, 16181–16196.
6. W. C. Yount, D. M. Loveless and S. L. Craig, *J. Am. Chem. Soc.*, 2005, **127**, 14488–14496.
7. E. A. Appel, R. A. Forster, A. Koutsioubas, C. Toprakcioglu and O. A. Scherman, *Angew. Chem., Int. Ed.*, 2014, **53**, 10038–10043.
8. Y.-C. Yu, P. Berndt, M. Tirrell and G. B. Fields, *J. Am. Chem. Soc.*, 1996, **118**, 12515–12520.
9. D. D. McKinnon, D. W. Domaille, J. N. Cha and K. S. Anseth, *Adv. Mater.*, 2014, **26**, 865–872.
10. V. Yesilyurt, M. J. Webber, E. A. Appel, C. Godwin, R. Langer and D. G. Anderson, *Adv. Mater.*, 2016, **28**, 86–91.
11. N. van Herck, D. Maes, K. Unal, M. Guerre, J. M. Winne and F. E. du Prez, *Angew. Chem., Int. Ed.*, DOI:10.1002/anie.201912902.
12. S. C. Grindy, R. Learsch, D. Mozhdehi, J. Cheng, D. G. Barrett, Z. Guan, P. B. Messersmith and N. Holten-Andersen, *Nat. Mater.*, 2015, **14**, 1210–1216.
13. T. F. Scott, A. D. Schneider, W. D. Cook and C. N. Bowman, *Science*, 2005, **308**, 1615–1617.
14. D. Montarnal, M. Capelot, F. Tournilhac and L. Leibler, *Science*, 2011, **334**, 965–968.
15. W. Denissen, J. M. Winne and F. E. du Prez, *Chem. Sci.*, 2016, 7, 30–38.
16. J. P. Brutman, P. A. Delgado and M. A. Hillmyer, *ACS Macro Lett.*, 2014, **3**, 607–610.
17. Y. Zhou, J. G. P. Goossens, S. van den Bergen, R. P. Sijbesma and J. P. A. Heuts, *Macromol. Rapid Commun.*, 2018, **39**, 1800356.
18. X. Niu, F. Wang, X. Li, R. Zhang, Q. Wu and P. Sun, *Ind. Eng. Chem. Res.*, 2019, **58**, 5698–5706.
19. Y.-X. Lu, F. Tournilhac, L. Leibler and Z. Guan, *J. Am. Chem. Soc.*, 2012, **134**, 8424–8427.
20. H. Liu, A. Z. Nelson, Y. Ren, K. Yang, R. H. Ewoldt and J. S. Moore, *ACS Macro Lett*, 2018, **7**, 933–937.
21. M. Röttger, T. Domenech, R. van der Weegen, A. Breuillac, R. Nicolaÿ and L. Leibler, *Science*, 2017, **356**, 62–65.
22. A. Breuillac, A. Kassalias and R. Nicolaÿ, *Macromolecules*, 2019, **52**, 7102–7113.
23. F. Caffy and R. Nicolaÿ, *Polym. Chem.*, 2019, **10**, 3107–3115.
24. Y. Nishimura, J. Chung, H. Muradyan and Z. Guan, *J. Am. Chem. Soc.*, 2017, **139**, 14881–14884.

25. W. Denissen, M. Droesbeke, R. Nicola, L. Leibler, J. M. Winne and F. E. du Prez, *Nat. Commun.,* 2017, **8**, 4857.

26. W. Denissen, G. Rivero, R. Nicolaÿ, L. Leibler, J. M. Winne and F. E. du Prez, *Adv. Funct.l Mater.*, 2015, **25**, 2451–2457.

27. D. J. Fortman, J. P. Brutman, C. J. Cramer, M. A. Hillmyer and W. R. Dichtel, *J. Am. Chem. Soc.*, 2015, **137**, 14019–14022.

28. R. L. Snyder, D. J. Fortman, G. X. de Hoe, M. A. Hillmyer and W. R. Dichtel, *Macromolecules*, 2018, **51**, 389–397.

29. C. He, S. Shi, D. Wang, B. A. Helms and T. P. Russell, *J. Am. Chem. Soc.*, 2019, **141**, 13753–13757.

30. H. Geng, Y. Wang, Q. Yu, S. Gu, Y. Zhou, W. Xu, X. Zhang and D. Ye, *ACS Sustain. Chem. Eng.*, 2018, **6**, 15463–15470.

31. T. Stukenbroeker, W. Wang, J. M. Winne, F. E. du Prez, R. Nicolaÿ and L. Leibler, *Polym. Chem.*, 2017, **8**, 6590–6593.

32. Z. Ma, Y. Wang, J. Zhu, J. Yu and Z. Hu, *J. Polym. Sci., Part A: Polym. Chem.*, 2017, **55**, 1790–1799.

33. J. Tellers, R. Pinalli, M. Soliman, J. Vachon and E. Dalcanale, *Polym. Chem.*, 2019, **10**, 5534–5542.

34. D. J. Fortman, J. P. Brutman, M. A. Hillmyer and W. R. Dichtel, *J. Appl. Polym. Sci.*, 2017, **134**, 44984.

35. C. Taplan, M. Guerre, J. M. Winne and F. E. du Prez, *Mater. Horiz.*, DOI:10.1039/c9mh01062a.

36. T. E. Brown, B. J. Carberry, B. T. Worrell, O. Y. Dudaryeva, M. K. McBride, C. N. Bowman and K. S. Anseth, *Biomaterials*, 2018, **178**, 496–503.

37. B. T. Worrell, S. Mavila, C. Wang, T. M. Kontour, C. H. Lim, M. K. McBride, C. B. Musgrave, R. Shoemaker and C. N. Bowman, *Polym. Chem.*, 2018, **9**, 4523–4534.

38. M. Capelot, M. M. Unterlass, F. Tournilhac and L. Leibler, *ACS Macro Lett.*, 2012, **1**, 789–792.

39. J. L. Self, N. D. Dolinski, M. S. Zayas, J. Read de Alaniz and C. M. Bates, *ACS Macro Lett.*, 2018, **7**, 817–821.

40. K. L. Diehl, I. v. Kolesnichenko, S. A. Robotham, J. L. Bachman, Y. Zhong, J. S. Brodbelt and E. v. Anslyn, *Nat. Chem.*, 2016, **8**, 968–973.

41. J. S. A. Ishibashi and J. A. Kalow, *ACS Macro Lett.*, 2018, **7**, 482–486.

42. M. Guerre, C. Taplan, R. Nicolaÿ, J. M. Winne and F. E. du Prez, *J. Am. Chem. Soc.*, 2018, **140**, 13272–13284.

43. B. B. Jing and C. M. Evans, *J. Am. Chem. Soc.*, 2019, **141**, 18932–18937.

44. V. Yesilyurt, A. M. Ayoob, E. A. Appel, J. T. Borenstein, R. Langer and D. G. Anderson, *Adv. Mater.*, 2017, **29**, 1605947.

45. L. J. Dooling and D. A. Tirrell, *ACS Cent. Sci.*, 2016, **2**, 812–819.